Water **2015**, *7*, 1515-1537; doi:10.3390/w7041515

OPEN ACCESS

water

ISSN 2073-4441

www.mdpi.com/journal/water

Article

Evaluating the Sources and Fate of Nitrate in the Alluvial Aquifers in the Shijiazhuang Rural and Suburban Area, China: Hydrochemical and Multi-Isotopic Approaches

Yanpeng Zhang [1,2], Aiguo Zhou [1,2], Jianwei Zhou [1,2,*], Cunfu Liu [1], Hesheng Cai [1], Yunde Liu [1,2] and Wen Xu [1,2]

[1] School of Environmental Studies, China University of Geosciences, Wuhan 430074, China; E-Mails: yanpeng1028@126.com (Y.Z.); aiguozhou0516@126.com (A.Z.); cfliu101@126.com (C.L.); hshcai@cug.edu.cn (H.C.); lydcn84@126.com (Y.L.); xuwen8971@163.com (W.X.)

[2] State Key Laboratory of Biogeology and Environmental Geology (China University of Geosciences), Wuhan 430074, China

* Author to whom correspondence should be addressed; E-Mail: jw.zhou@cug.edu.cn; Tel.: +86-27-6788-3473.

Academic Editor: Jun Xu

Received: 7 December 2014 / Accepted: 27 March 2015 / Published: 9 April 2015

Abstract: The identification of the sources and fate of NO_3^- contaminants is important to protect the water quality of aquifer systems. In this study, NO_3^- contaminated groundwater from the drinking water wells in the Shijiazhuang area, China, was chemically (NO_3^-/Cl^- ratio) and isotopically ($\delta^{15}N_{NO3}$, $\delta^{18}O_{NO3}$ and $\delta^{13}C_{DOC}$; $\delta^{2}H_{H2O}$, $\delta^{18}O_{H2O}$) characterized to identify the sources of NO_3^- and address subsequent biogeochemical processes. The positive correlations between dominant anions and cations suggested that the dissolution of calcium carbonate and gypsum minerals was the most effective process in the groundwater. Elevated concentrations of NO_3^-, Cl^- and Mg^{2+} could be related to the wastewater irrigation and usage of fertilizers. The natural water in the study area originated primarily from precipitation and experienced a limited extent of evaporation, as demonstrated by measurements of $\delta^{2}H_{H2O}$ and $\delta^{18}O_{H2O}$. A cross-plot of $\delta^{15}N_{NO3}$ *vs.* $\delta^{18}O_{NO3}$ gave an enrichment of the ^{15}N isotope relative to the ^{18}O isotope by a factor of 2. A further insight into the denitrification process was obtained by the synergistic changes in $\delta^{13}C_{DOC}$ and $\delta^{15}N_{NO3}$ values, confirming that a low extent of denitrification occurred. Nitrification processes were evaluated by means of $\delta^{18}O_{NO3}$ and $\delta^{18}O_{H2O}$. The initial $\delta^{15}N_{NO3}$ value(s) of the NO_3^- source(s) were roughly estimated between 2‰ and 5‰. Based on the level of natural NO_3^-, anthropogenic activities were

considered the main reason for the elevated NO_3^- concentration of the shallow groundwater. NH_4^+ fertilizers were the major source of NO_3^- in the non-wastewater irrigated area, while wastewater was regarded as the primary source of NO_3^- in the wastewater-irrigated area. A low content of NO_3^- in deep groundwater might mainly be influenced by precipitation and soil organic N that was involved in denitrification reactions. Some of the deep groundwater samples could have been contaminated by wastewater. The mixing process of multiple NO_3^- sources was identified as another important factor affecting the NO_3^- concentration of the groundwater in the study area. The combined use of $\delta^{15}N_{NO3}$, $\delta^{18}O_{NO3}$ and $\delta^{13}C_{DOC}$ results and hydrochemical data (NO_3^-/Cl^- ratios) gives an insight into the mixing effect of different NO_3^- sources and processes affecting NO_3^- concentration under conditions of intensive land-use activities.

Keywords: groundwater; nitrate sources; denitrification; multiple isotopes

1. Introduction

Shijiazhuang (SJZ) City is a representative area, which has been developed from a rural area to a metropolitan city in China. In most suburban and rural regions of SJZ, groundwater is the major source of drinking water due to the inadequate centralized water supply system. Nitrate contamination in groundwater caused by intensive land-use activities has become a major environmental concern in this area [1,2]. To prevent the deterioration of groundwater quality due to nitrate contamination, it is important to discern the major sources and fate of nitrate [3–5].

Some studies have been conducted to identify the nitrate contamination of groundwater using stable isotopes near the city of SJZ [6–8]. In the wastewater-irrigated area (the southern part of the study area), a stable N isotope of nitrate indicated that the nitrate in the groundwater originated from wastewater or a mixture of pig manure and wastewater [6,8]. However, the single isotope approach applied in these studies could not fully interpret the transformation of nitrogen in the groundwater. In the non-wastewater-irrigated area, a combination of $\delta^{15}N_{NO3}$ and $\delta^{18}O_{NO3}$ was used to trace NO_3^- sources in the shallow groundwater, suggesting that NH_4^+ fertilizer and manure were the main sources of NO_3^- in the groundwater; nevertheless, denitrification seriously interfered with determining the source of nitrate [7].

In addition, previous studies drew different conclusions on whether microbial denitrification occurred. Chen *et al*., found a good linear relationship of $\delta^{15}N$ and the logarithm of the residual NO_3^- that was consistent with denitrification of NO_3^- in groundwater in the southern part of the study area [6]. Similarly, Liu and Chen observed a linear relationship with a slope of 0.644 ($\varepsilon N/\varepsilon O = 1.5$) between $\delta^{15}N_{NO3}$ and $\delta^{18}O_{NO3}$ values (4.6‰–9.7‰ and 2.3‰–7.8‰, respectively) confirming the occurrence of denitrification [7]. Others, however, suggested the absence of denitrification based on constant NO_3^-/Cl^- values, high DO values (1.20–5.97 mg/L) and a limited range of $\delta^{15}N_{NO3}$ values [8]. In general, it is difficult to specify the varied sources and processes that affect the isotope composition of NO_3^- due to the isotope fractionation combined with similar isotopic values of various NO_3^- sources in SJZ area.

Similarly, isotopic composition of nitrate used to constrain the sources and fate of N also appears to have certain limitation in other study cases [4,5,9,10]. $\delta^{15}N_{NO3}$ was not sufficient to estimate potential

sources of nitrate contamination in rural regions in Korea since the concentration and $\delta^{15}N_{NO3}$ of the unconfined groundwater nitrate exhibited seasonal variations due to seasonal changes in agricultural activities [11]. Later, the same author proposed that the impacts of various land-use activities on the nitrate contamination of groundwater could be more precisely inferred from long-term data on the concentration and $\delta^{15}N_{NO3}$ of nitrate [12]. Since denitrification and mixing processes limited the identification of NO_3^- sources by $\delta^{15}N_{NO3}$ in the groundwater, $\delta^{15}N_{NO3}$ was combined with co-migrating isotopic tracers ($\delta^{11}B$ and $^{87}Sr/^{86}Sr$) to distinguish various NO_3^- sources under intensive agricultural activities in Brittany (France) [13]. In addition, based on the level of natural NO_3^- in the groundwater, anthropogenic contamination (inorganic fertilizer) can be discriminated from the soil organic N using $\delta^{15}N_{NO3}$ and $\delta^{18}O_{NO3}$ isotopic values in the Mt. Vulture area (Italy) [14]. These studies indicated that, for better understanding of the various sources and transformations of NO_3^- in groundwater, it is important to couple isotopic composition of NO_3^- with multiple lines of evidence.

Dissolved organic carbon (DOC) is ubiquitous in groundwater [15]. Changes in concentration and composition of DOC reflect biogeochemical sources and reaction processes that determine the chemical composition of groundwater [16–18]. Numerous studies have described the importance of organic carbon in controlling the occurrence of denitrification. Several studies relate denitrification activity to DOC concentration [19,20]. The availability of organic carbon limits the denitrification rate [17,21–24]. On the other hand, biogeochemical activities can be inferred from elevated $\delta^{13}C_{DOC}$ values [25,26]. Breukelen *et al*., found that dissolved organic carbon (DOC) concentration decreased in association with increasing $\delta^{13}C_{DOC}$ values in a landfill leachate plume, supporting the occurrence of degradation and denitrification potentially being the dominated redox process at the top fringe [27]. It is hypothesized that the combination of $\delta^{13}C_{DOC}$ and $\delta^{15}N_{NO3}$ isotopic values would provide a sensitive method for tracing denitrification process in groundwater.

The NO_3^-/Cl^- method has been proven to be a valid and effective tool to distinguish the effect of N removal processes by dilution from denitrification [28,29]. In addition, the NO_3^-/Cl^- in groundwater can be used as a source indicator because different sources of nitrate and chloride have different ratios in most cases [18,30]. Nishikawa *et al*., reported that the NO_3^-/Cl^- ratios for the native groundwater, imported water, and septage collected in Warren ground-water basin were completely different. Based on the NO_3^-/Cl^- ratios and NO_3^- concentrations, a three-part mixture of native ground water, imported water, and septage was identified [18]. Liu *et al*., showed the variation of the NO_3^-/Cl^- molar ratios with Cl^- concentrations in the surface and groundwater samples as well as sewage samples in both the summer and winter seasons [30]. Two NO_3^- source end members were distinguished as agricultural inputs with low-Cl/high-NO_3^-/Cl^- ratios and municipal inputs with high-Cl/low-NO_3^-/Cl^- ratios close to sewage.

In this study, the characteristics of $\delta^{15}N_{NO3}$, $\delta^{18}O_{NO3}$, and $\delta^{13}C_{DOC}$ were investigated in the unconfined Quaternary aquifers of SJZ, China. Traditional hydrochemical and isotopic parameters such as chemical composition (anion, cation, DOC concentrations and NO_3^-/Cl^- ratio), $\delta^2H_{H2O,}$ and $\delta^{18}O_{H2O}$ of groundwater were also measured. The aim of this study is to combine $\delta^{15}N_{NO3}$, $\delta^{18}O_{NO3}$, and $\delta^{13}C_{DOC}$ data with the NO_3^-/Cl^- ratio to understand biogeochemical processes in an alluvial aquifer where there are multiple potential NO_3^- sources, and to identify the mixing process of different NO_3^- sources in this region.

2. Materials and Methods

2.1. Description of the Study Area

The Shijiazhuang (SJZ) area is located in the piedmont pluvial plain of Hutuo River (Figure 1). The region is middle-latitude continental semiarid monsoon climate with mean annual temperature of 12–13 °C, mean annual precipitation of 500–600 mm, and potential evaporation of 1100–1800 mm [31,32]. Historically, the Hutuo River played an important role in the formation of the alluvial fan at the front edge of the piedmont plain zone in the study area [33]. Today, the river is disconnected and severed due to drought and interception of water by the Huangbizhuang reservoir. The Shijin and Dongming canals are mainly used for agricultural irrigation. Xiao River is a seasonal stream originating from a mountainous area. Over the past few decades, a quantity of industrial and domestic wastewater flowed into Xiao River through Dongming Canal.

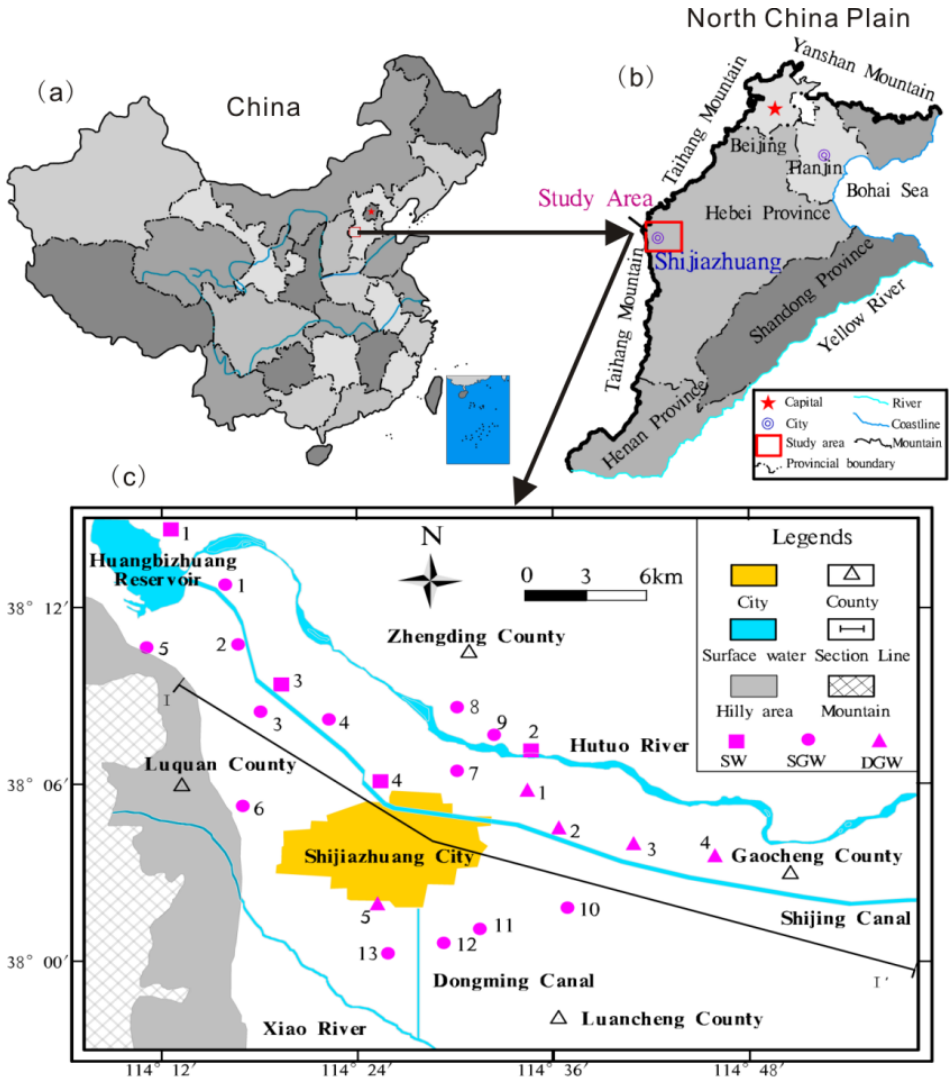

Figure 1. Illustration of the study area and sampling points. (**a**,**b**) are location maps of the study area; and (**c**) sampling map. Line I–I' indicates location of hydrogeologic cross section in Figure 2. (SW: Surface water; SGW: Shallow groundwater; DGW: Deep groundwater).

The aquifers in this area are mainly composed of the multi-layer loose deposits of Quaternary with a depth of 350–450 m in the piedmont (Figure 2). The regional Quaternary aquifers can be divided into four groups: The Holocene formation (Q4), the late Pleistocene formation (Q3), the middle Pleistocene formation (Q2), and the early Pleistocene formation (Q1) [34]. Aquifer 1 (A1) is an unconfined shallow aquifer dominated by coarse-grained sand with the bottom boundary at 10–20 m deep, in which groundwater has been drained. Aquifer 2 (A2), a 50 m thick shallow confined aquifer (30–80 m depth), contains sandy gravel and medium to fine sand, and is the main source of groundwater for drinking water supplies. Aquifers 3 (A3) and 4 (A4) are both deep confined aquifers, consisting of 90 m thick sandy gravel (80–200 m depth) and 50–60 m thick cemented sandy gravel (300–370 m depth), respectively [1,34]. The shallow aquifers (A1 and A2) can be regarded as one system as a result of the natural hydraulic connection between them [31]. Aquifers 3 and 4 can be recognized as the deep unit. The shallow aquifers are over developed and contaminated, increasing the need to pump clean groundwater from the deep aquifers.

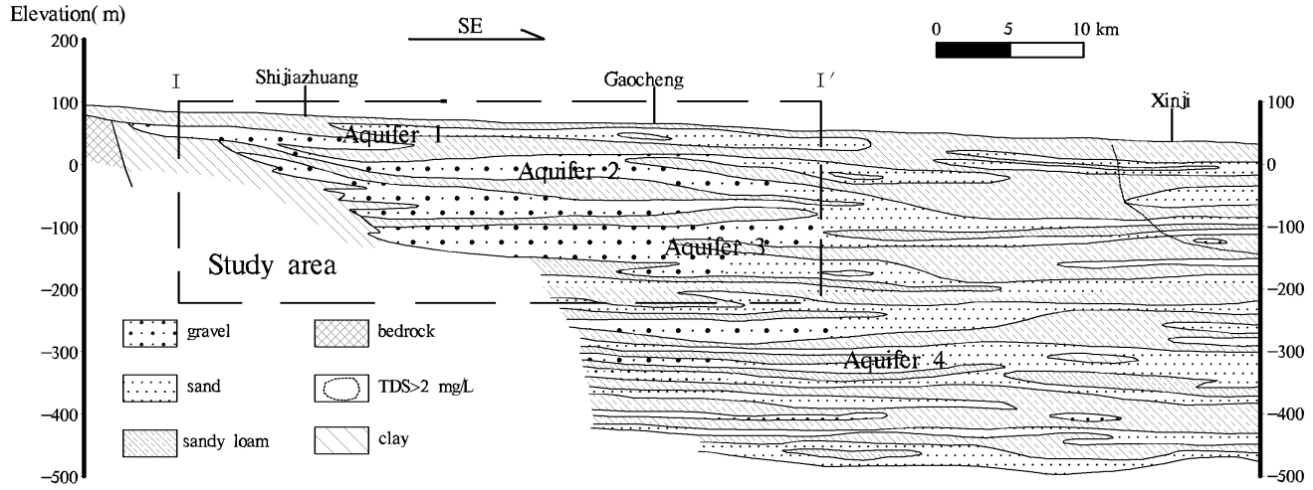

Figure 2. The hydrogeologic cross section in Shijiazhuang. The range of study area is marked by rectangle with dashed lines. The Quaternary aquifers are divided into four groups named as Aquifers 1–4.

Several components make up groundwater recharge in the shallow groundwater aquifer unit: Precipitation, irrigation return flow, infiltration of surface water in rivers and canals, and lateral inflow from the Taihang Mountains [35]. The deep aquifer is mainly recharged by infiltration of paleo-precipitation under cold climatic conditions with modern vertical inflow from the shallow aquifer as another source.

Currently, groundwater discharge in the study area is mainly through intensive localized pumping in SJZ City and widespread pumping via small capacity wells for irrigation in the surrounding country areas [31,32,36]. Groundwater exploitation has resulted in serious water-level decline, forming a 400 km^2 groundwater cone of depression in the shallow aquifer [37,38]. The water table is currently more than 10 m below ground surface; thus, evaporation of groundwater is generally considered negligible [39].

2.2. Sampling and Analytical Methods

Groundwater samples from domestic wells and surface water samples from the Huangbizhuang reservoir, Hutuo River and Shijin Canal were collected in September 2011 (Figure 1). Samples were collected unacidified for analysis of concentrations and values for anion, deuterium, and oxygen isotopes. Samples were acidified to pH < 2 with concentrated HNO_3 for cation analysis. To obtain sufficient dissolved NO_3^- for N and O isotope analyses, five liters of water were taken from each sampling site. For dissolved organic carbon (DOC) concentration and C isotope analysis, 500 mL water samples were collected in amber glass bottles. All these samples were stored below 4 °C and transferred to the lab for chemical and isotopic analyses. The temperature, pH values and electrical conductivity (EC) were measured on site. Alkalinity was determined by titration within 24 h after sampling. Samples were filtered through 0.45 μm membrane filters prior to measurement of ion and DOC concentration, and C, N, O and H isotopic analyses. All these measurements were performed at China University of Geosciences (Wuhan), China.

The concentrations of major cations and anions were measured by inductively coupled plasma-atomic emission spectrometry (ICAP6300, ICP-OES, Thermo Jarrell Ash Co., Franklin, MA, USA) and ion chromatography (Dionex ICS-1100, Dionex Co, Sunnyvale, CA, USA), respectively. DOC concentrations were determined using a TOC/TN analyzer (Analytik Jena AG, Jena, Germany).

All stable isotopic compositions are reported in per mil relative to their corresponding international standards (VPDB for ^{13}C, V-SMOW for ^{2}H and ^{18}O, AIR for ^{15}N), using the delta notation: $\delta(‰) = [(R - R_{std})/R_{std}] \times 1000$, where R and R_{std} are the isotope ratio of the sample and the standard, respectively.

O and H isotopic compositions were determined by a Thermal Conversion Elemental Analyzer (TC/EA, Thermo Finnigan, Bremen, Germany) coupled with the MAT 253 (Thermo Finnigan) [40], with a precision of ±0.1‰ and ±1‰ for $\delta^{18}O_{H2O}$ and $\delta^{2}H_{H2O}$, respectively.

For analysis of N and O isotopes in nitrate, a modification of the procedure described by Silva (2000) was used for the conversion of dissolved NO_3^- to $AgNO_3$ salt [41]. The water samples were filtered through 0.45 μm membrane filters in the laboratory. The Barium chloride was added to precipitate sulfate and phosphate in 5 L samples. Then the solution was filtered, agitated with activated carbon to remove dissolved organic matters, passed through a cation exchange column to remove all cations, neutralized with Ag_2O, filtered to remove the AgCl precipitate, and freeze-dried to obtain solid $AgNO_3$ [41]. About 0.5 mg $AgNO_3$ was transferred to silver capsules and loaded into the auto-sampler coupled to the EA (Flash 2000, Thermo Finnigan). N_2 and CO generated after $AgNO_3$ pyrosis at 1325 °C were separated in a chromatographic column at 60 °C, and then introduced into MAT 253 (Thermo Finnigan) where $\delta^{15}N_{NO3}$ and $\delta^{18}O_{NO3}$ were determined with a total uncertainty of ±0.3‰ for $\delta^{15}N_{NO3}$ and of ±0.5‰ for $\delta^{18}O_{NO3}$, respectively, for solutions of KNO_3 standard processed through the entire column procedure.

To measure the C isotope of DOC, 200 mL water from each sample was concentrated to a volume of about 1 mL at 40 °C in a round-bottomed flask by rotary evaporation, and then acidified to pH 2 by adding 2–3 drops of 85% phosphoric acid to remove the dissolved inorganic carbon (DIC) by agitation. Flask was rinsed with two 1.5 mL aliquots of ultra-pure deionized water, resulting in a final volume of 3.5–4.5 mL. One hundred μL of the concentrated sample was transferred to silver capsules (8 mm × 5 mm) and dried at 70 °C. More details about the procedure for preparation were described in a previous study [42].

The $\delta^{13}C_{DOC}$ analyses was carried out using a MAT 253 (Thermo Finnigan) after combustion in a Flash EA via open split at a temperature of 1020 °C, with a precision of ±0.25‰.

3. Results

3.1. Chemical Composition

The geochemical parameters and major ion composition of surface water (SW), shallow groundwater (SGW), and deep groundwater (DGW) samples are summarized in Table 1. Chemical data obtained are also plotted on a Piper diagram (Figure 3).

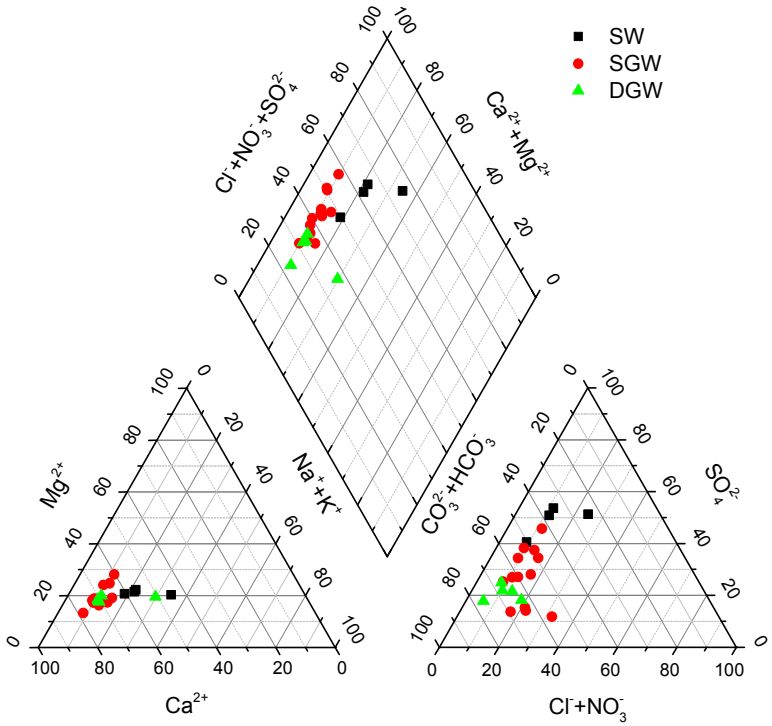

Figure 3. Piper diagram of water samples. (SW: Surface water; SGW: Shallow groundwater; DGW: Deep groundwater).

The SW samples were alkaline with a pH of 8.1 to 9.2. Water temperatures ranged from 18 to 26 °C. Electrical conductivities (EC) varied from 577 to 717 µS/cm. Concentrations of dissolved organic carbon (DOC) in the SW samples ranged from 4.1 to 22.1 mg C/L. The dissolved oxygen (DO) in SW01 and SW03 were 4.7 and 4.8 mg/L, respectively, while the DO concentration in SW02 was lower (2.3 mg/L). The concentrations of cations and anions in most SW samples followed the order: $Ca^{2+} > Mg^{2+} > Na^{+} + K^{+}$ and $SO_4^{2-} > HCO_3^{-} > Cl^{-} + NO_3^{-}$, except anions in the sample SW4 ($HCO_3^{-} > SO_4^{2-} > Cl^{-} + NO_3^{-}$).

Table 1. Chemical compositions and field data of the surface water and groundwater in Shijiazhuang.

Sample	Site Description	Depth (m)	T (°C)	pH	EC (μS/cm)	DOC (mg C/L)	DO	K^+	Na^+	Ca^{2+}	Mg^{2+}	Cl^-	SO_4^{2-}	NO_3^-	HCO_3^-	Chemical Type
							(mg/L)									
Surface Water																
SW1	HBZ Reserior	–	18	8.4	689	4.1	4.7	4.3	22.7	69.6	27.6	57.2	263.3	2.6	194.7	SO_4-HCO_3-Ca-Mg
SW2	Hutuo River	–	19	9.2	715	22.1	2.3	10.4	35.6	59.9	27.0	104.2	222.7	2.1	105.3	SO_4-HCO_3-Ca-Mg
SW3	Shijin Canal	–	22	8.5	717	6.3	4.8	4.4	23.1	72.3	27.3	55.1	266.1	2.6	172.5	SO_4-HCO_3-Ca-Mg
SW4	Shijin Canal	–	26	8.1	577	14.2	*n.d.*	4.6	17.5	71.4	24.4	37.6	178.2	2.3	221.2	HCO_3-SO_4-Ca-Mg
Shallow Groundwater																
SGW1	Yancun	34	24	7.6	906	4.2	2.6	1.6	20.0	125.1	28.5	52.2	232.6	10.7	380.5	HCO_3-SO_4-Ca-Mg
SGW2	Baichigan	40	20	7.4	928	3.9	2.5	1.8	16.8	133.3	31.9	65.6	192.6	13.3	442.4	HCO_3-SO_4-Ca-Mg
SGW3	Dahe	40	19	7.2	1179	4.7	2.9	1.4	20.1	171.4	42.8	119.5	302.5	21.4	433.6	HCO_3-SO_4-Ca-Mg
SGW4	Houdubei	45	26	7.6	808	4.6	*n.d.*	1.8	21.0	105.7	26.9	48.9	227.0	6.5	310.6	HCO_3-SO_4-Ca-Mg
SGW5	Shiqiyu	60	17	7.3	970	20.2	2.2	1.9	20.1	162.5	38.7	68.6	332.7	16.2	309.7	SO_4-HCO_3-Ca-Mg
SGW6	Taitou	15	16	7.1	1199	10.2	2.2	0.5	23.0	215.1	36.5	108.2	350.2	15.6	460.1	HCO_3-SO_4-Ca-Mg
SGW7	Beigaoying	60	21	7.2	1005	4.8	2.0	2.2	16.4	140.5	36.9	65.3	192.1	26.2	424.7	HCO_3-SO_4-Ca-Mg
SGW8	Xiguan	50	23	7.4	986	5.7	3.1	3.2	20.1	137.4	36.3	57.3	227.5	22.3	592.8	HCO_3-SO_4-Ca-Mg
SGW9	Taipingcun	60	22	7.6	920	9.6	2.5	2.9	18.5	140.2	37.1	92.9	184.7	17.3	362.8	HCO_3-SO_4-Ca-Mg
SGW10	Bafang	60	19	7.4	795	5.3	1.8	2.3	13.4	104.1	38.0	95.2	80.5	5.7	407.0	HCO_3-Cl-Ca-Mg
SGW11	Dongxuying	60	24	7.3	1007	9.9	1.1	2.2	20.6	123.7	48.0	142.9	108.8	7.7	451.2	HCO_3-Cl-Ca-Mg
SGW12	Shaojiazhuang	40	17	7.1	1189	15.8	2.8	2.0	24.9	140.7	65.6	254.0	102.2	23.2	486.6	HCO_3-Cl-Ca-Mg
SGW13	Gaoqianbeijie	60	17	7.0	1188	4.8	1.2	1.1	36.1	159.1	46.3	174.7	121.3	15.1	548.6	HCO_3-Cl-Ca-Mg
Deep Groundwater																
DGW1	Xizhaotong	100	23	7.9	589	3.9	2.5	1.5	13.5	90.2	22.5	33.5	112.5	4.8	300.8	HCO_3-SO_4-Ca-Mg
DGW2	Wujiaying	100	17	7.6	537	4.3	1.5	1.2	11.6	82.1	21.0	42.8	97.0	3.1	300.8	HCO_3-SO_4-Ca-Mg
DGW3	Liangcun	125	18	7.7	507	3.1	1.8	1.3	11.1	80.8	21.2	52.8	85.6	1.8	256.6	HCO_3-SO_4-Ca-Mg
DGW4	Nandun	150	20	7.8	464	3.3	2.0	1.7	9.6	68.3	19.8	22.3	68.2	0.5	292.0	HCO_3-SO_4-Ca-Mg
DGW5	Tatan	180	20	7.5	994	5.5	2.6	1.2	49.8	87.0	33.5	121.7	125.1	5.9	433.6	HCO_3-SO_4-Ca-Mg

Notes: T, temperature; EC, electrical conductivity; DOC, dissolved organic carbon; DO, dissolved oxygen; *n.d.*, not determined.

The pH values of SGW samples ranged from 7.0 to 7.6, and temperatures ranged from 16 to 26 °C. Conductivities varied from 795 to 1199 μS/cm. The DOC concentrations of most SGW samples varied in the range of 3.9 to 10.2 mg C/L, except for samples of SGW5 and SGW12 with values of 20.2 and 15.8 mg C/L, respectively. The DO concentration in SGW samples ranged from 1.1 to 3.1 mg/L. The orders of dominant cations and anions in SGW samples were $Ca^{2+} > Mg^{2+} > Na^+ + K^+$ and $HCO_3^- > SO_4^{2-} > Cl^- + NO_3^-$, except the order of anion in sample SGW5 was $SO_4^{2-} > HCO_3^- > Cl^- + NO_3^-$ and in SGW10-13 was $HCO_3^- > Cl^- + NO_3^- > SO_4^{2-}$. In particular, the HCO_3.Cl-Ca.Mg type of groundwater was generally found in the southeastern part of the study area where the wastewater was used for irrigation during the1960s to 2000s [6].The DGW samples had pH values of 7.5 to 7.9 and temperatures between 17 and 23 °C. Most samples had low conductivities ranging from 464 to 589 μS/cm, whereas sample DGW5 had a high value of 994 μS/cm. The DGW samples had relatively low DOC concentrations in a narrow range of 3.1 to 5.5 mg C/L. The DO concentration in DGW samples ranged from 1.5 to 2.6 mg/L. The orders of dominance of cations and anions in DGW samples were $Ca^{2+} > Mg^{2+} > Na^+ + K^+$ and $HCO_3^- > SO_4^{2-} > Cl^- + NO_3^-$.

NO_3^- concentrations of local surface water and groundwater varied significantly. Concentrations of NO_3^- in SW samples varied in a narrow range from 2.1 to 2.6 mg/L. The contents of NO_3^- in the SGW and DGW samples were determined in the range of 5.7 to 26.2 mg/L (average 15.5 mg/L) and 0.5 to 5.9 mg/L (average 3.2 mg/L), respectively. All samples had lower NO_3^- content than the statutory limit (50 mg/L for NO_3^-) for drinking water (GB5749). However, the NO_3^- concentrations of most groundwater samples were significantly higher than the regional background value (4.4 mg/L in 1950s) in the groundwater.

3.2. Isotope Data

The isotopic compositions of NO_3^-, DOC and H_2O in water samples from SJZ are presented in Table 2.

The $\delta^{15}N_{NO3}$ and $\delta^{18}O_{NO3}$ values in the SW samples were in the range of 9.4‰ to 12.6‰ and 10.9‰ to 20.2‰, respectively. The SGW samples had $\delta^{15}N_{NO3}$ values ranging from 7.1‰ to 11.3‰ (average 8.8‰), and $\delta^{18}O_{NO3}$ values ranging from 5.4‰ to 11.6‰ (average 8.4‰). $\delta^{15}N_{NO3}$ values of DGW samples ranging from 9.4‰ to 11.9‰ (average 10.4‰), were higher than most of the SGW samples (except SGW6, SGW11 and SGW13). $\delta^{18}O_{NO3}$ values of DGW samples ranged from 11.1‰ to 27.1‰ (average 20.1‰). The observed $\delta^{18}O_{NO3}$ values in DGW samples were more enriched than that of SGW samples.

The $\delta^{13}C_{DOC}$ values of SW samples showing wide ranges varied from −31.7‰ to −24.7‰ (average −28.6‰). The $\delta^{13}C_{DOC}$ values in SGW samples were in the range of −32.4‰ to −25.5‰ (average −29.5‰). The deep groundwater had relatively positive $\delta^{13}C_{DOC}$ values in a narrow range of −27.1‰ to −25.7‰ (average −26.1‰).

The isotope ratios of the surface water showed a range of −58‰ to −51‰ for δ^2H_{H2O} and −6.5‰ to −4.6‰ for $\delta^{18}O_{H2O}$, with negative d-excess values (d-excess = δ^2H_{H2O}-8$\delta^{18}O_{H2O}$) of −15.2‰ to 0‰. The δ^2H_{H2O} and $\delta^{18}O_{H2O}$ values of the shallow groundwater ranged from −64‰ to −53‰ and −8.5‰ to −6.0‰, respectively, with d-excess values varying in a large range of −12‰ to 8.4‰. The isotope ratios of the deep groundwater were generally lower than that of surface water and shallow groundwater,

ranging from −71‰ to −60‰ for δ^2H_{H2O} and from −9.8‰ to −8.0‰ for $\delta^{18}O_{H2O}$. The d-excess values displayed considerable variability ranging from −6.2‰ to 14.8‰.

Table 2. Environmental isotopes data of the field sampling.

Sample	Site Description	$\delta^{15}N_{NO3}$ (‰)	$\delta^{18}O_{NO3}$ (‰)	$\delta^{13}C_{DOC}$ (‰)	δ^2H_{H2O} (‰)	$\delta^{18}O_{H2O}$ (‰)	d-excess (‰)
Surface Water							
SW1	HBZ Reserior	12.6	20.2	−31.7	−58	−5.8	−11.6
SW2	Hutuo River	9.4	11.1	−26.6	−52	−4.6	−15.2
SW3	Shijin Canal	11.9	13.8	−31.2	−52	−6.5	0
SW4	Shijin Canal	11.7	10.9	−24.7	−51	−6.1	−2.2
Shallow Groundwater							
SGW1	Yancun	7.8	10.3	−32.2	−60	−6.0	−12
SGW2	Baichigan	7.8	6.2	−32.4	−56	−7.0	0
SGW3	Dahe	8.0	8.6	−32.2	−53	−7.1	3.8
SGW4	Houdubei	9.5	9.6	−30.9	−54	−6.9	1.2
SGW5	Shiqiyu	7.1	7.7	−32.3	−61	−8.5	7
SGW6	Taitou	11.1	11.6	−25.5	−56	−7.2	1.6
SGW7	Beigaoying	8.2	5.6	−28.1	−56	−7.0	0
SGW8	Xiguan	7.2	5.4	−27.3	−55	−7.3	3.4
SGW9	Taipingcun	9.3	6.7	−26.1	−64	−6.8	−9.6
SGW10	Bafang	9.1	11.5	−30.6	−58	−8.1	6.8
SGW11	Dongxuying	10.1	9.6	−28.6	−58	−8.2	7.6
SGW12	Shaojiazhuang	8.2	9.1	−31.7	−58	−8.3	8.4
SGW13	Gaoqianbeijie	11.3	7.4	−25.9	−59	−8.4	8.2
Deep Groundwater							
DGW1	Xizhaotong	9.4	24.8	−25.8	−60	−8.0	4
DGW2	Wujiaying	9.9	24.9	−27.1	−62	−9.6	14.8
DGW3	Liangcun	11.2	12.7	−25.9	−61	−8.1	3.8
DGW4	Nandun	11.9	27.1	−25.7	−71	−8.1	−6.2
DGW5	Tatan	9.6	11.1	−26.1	−69	−9.8	9.4

4. Discussion

4.1. Hydrochemical Characteristics of Water

Dissolution is the most effective process in groundwater chemistry and could be considered the first step in the hydrochemical evolution. As shown in Figure 4a,b, the molar ratios of Ca^{2+}/HCO_3^- are close to 0.5, while the molar ratios of $(Ca^{2+} + Mg^{2+})/HCO_3^-$ are greater than 0.5. This indicates that the dissolution of calcium carbonate minerals is one of the most important hydrochemical processes [43]. The linear correlations between Ca^{2+} and SO_4^{2-}, Na^+ and SO_4^{2-} suggest that SO_4^{2-} in groundwater may be mainly derived from the dissolution of gypsum and mirabilite (Figure 4c,d). High SO_4^{2-} concentration in the surface water might be the result of coal mining drainage from mountainous areas [36]. The shallow groundwater (HCO_3.Cl-Ca.Mg type) with low SO_4^{2-} concentration in the wastewater-irrigated area may be mainly affected by wastewater and precipitation (Figure 4c). The concentration of Mg^{2+} and Cl^- showed a linear relationship indicating that Mg^{2+} and Cl^- have a common source which could be attributed to

the anthropogenic activities such as wastewater irrigation or usage of fertilizers (Figure 4e) [6,28,44]. The plot of Na^+ and Cl^- shows that the increased Cl^- concentration is not closely related with the dissolution of halite or input of sea salt (Figure 4f).

In Figure 5a,b, NO_3^- concentrations show strong correlations with Mg^{2+} and Cl^- concentrations indicating that they originate from the same sources. The Mg^{2+} and Cl^- concentrations of the groundwater in the wastewater irrigation area were higher than those in the non-wastewater irrigated area, but the NO_3^- concentrations of groundwater in both areas fall within the similar range. This demonstrates that wastewater irrigation is not the only source of NO_3^- in groundwater. The concentrations of HCO_3^- and SO_4^{2-} are not correlated well with those of NO_3^- (Figure 5c,d), since the levels of HCO_3^- and SO_4^{2-} are controlled primarily by natural processes, and the concentration of NO_3^- is influenced mainly by anthropogenic inputs.

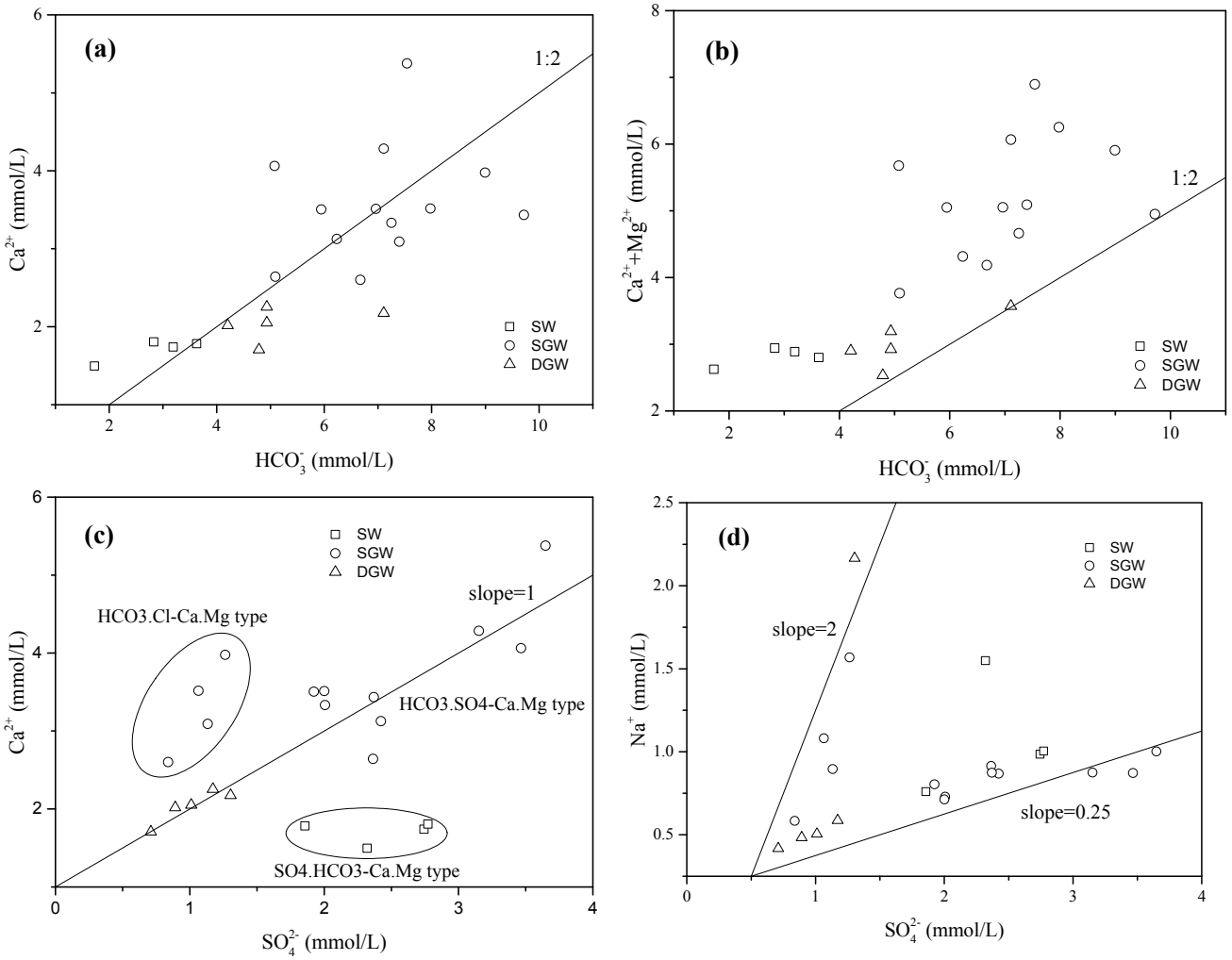

Figure 4. *Cont.*

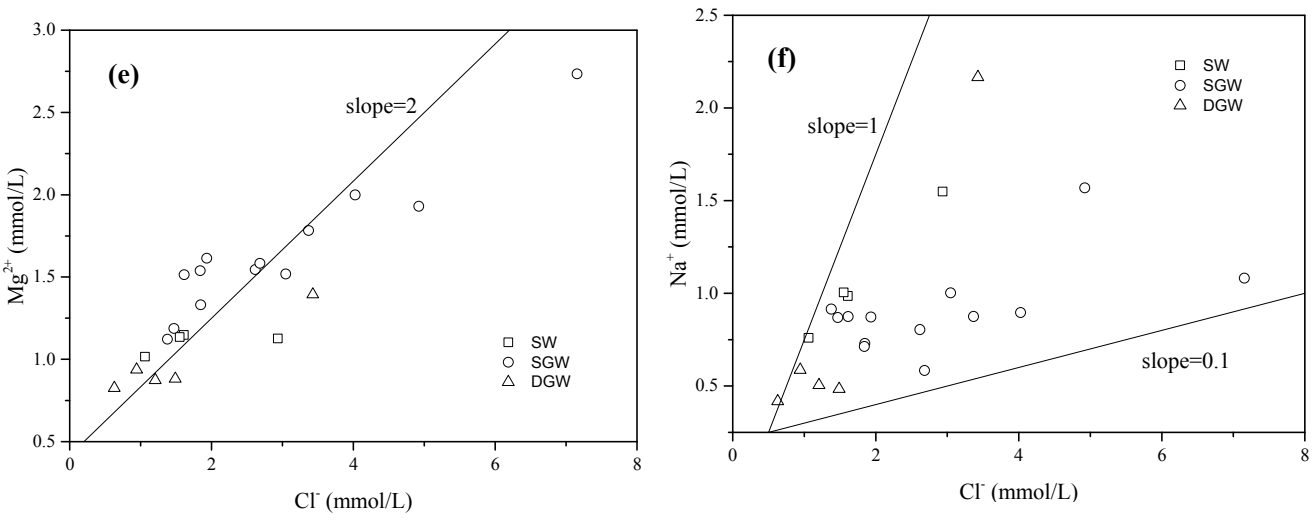

Figure 4. Relationships between ion concentrations of the surface water and groundwater, including (**a**) Ca^{2+} *vs.* HCO_3^-; (**b**) Ca^{2+}+Mg^{2+} *vs.* HCO_3^-; (**c**). Ca^{2+} *vs.* SO_4^{2-}; (**d**) Na^+ *vs.* SO_4^{2-}; (**e**) Mg^{2+} *vs.* Cl^-; and (**f**) Na^+ *vs.* Cl^-. (SW: Surface water; SGW: Shallow groundwater; DGW: Deep groundwater).

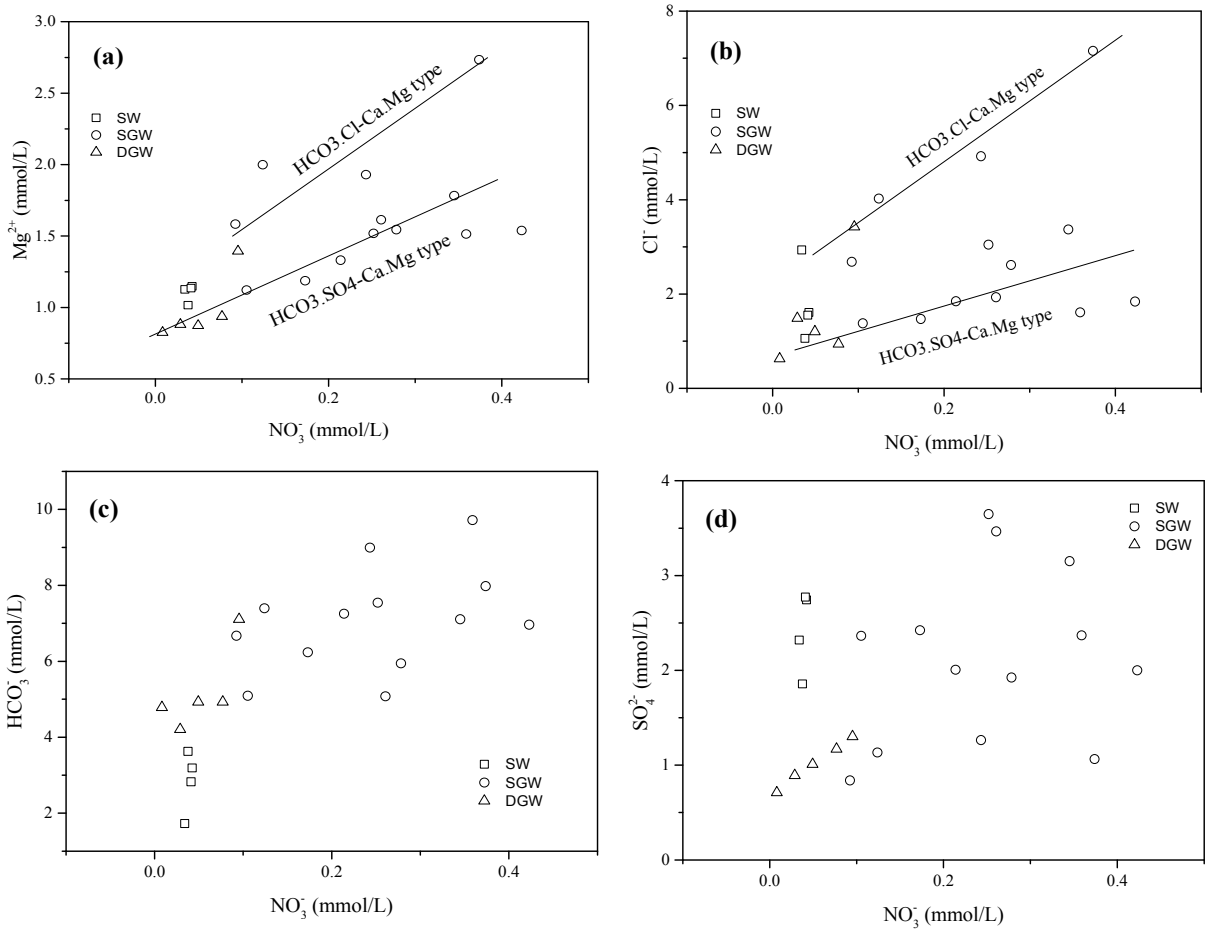

Figure 5. Concentrations of cation (Mg^{2+}) and anions (Cl^-, HCO_3^- and SO_4^{2-}) *vs.* that of NO_3^- concentrations in surface water and groundwater: (**a**) Mg^{2+} *vs.* NO_3^-; (**b**) Cl^- *vs.* NO_3^-; (**c**) HCO_3^- *vs.* NO_3^-; (**d**) SO_4^{2-} *vs.* NO_3^-. (SW: Surface water; SGW: Shallow groundwater; DGW: Deep groundwater).

The water samples all plot on or close to the local meteoric water line (LMWL) in Figure 6, suggesting that the surface water and groundwater originate from local precipitation. Most of the water samples have isotope compositions similar to the weighted mean isotope compositions (WMIC) of rain water in SJZ that has the composition of $\delta^2H_{H2O} = -55‰$ and $\delta^{18}O_{H2O} = -7.8‰$ (n = 142) calculated with data from 1985 to 2003 obtained from the Global Network for Isotopes in Precipitation (GNIP) dataset (available at http://isohis.iaea.org) (Figure 6). This isotopic similarity implies that the shallow groundwater was derived by direct inflow or infiltration of modern rainwater. The deep groundwater with relatively negative δ^2H_{H2O} and $\delta^{18}O_{H2O}$ reflects a paleorecharge effect under cold climatic conditions.

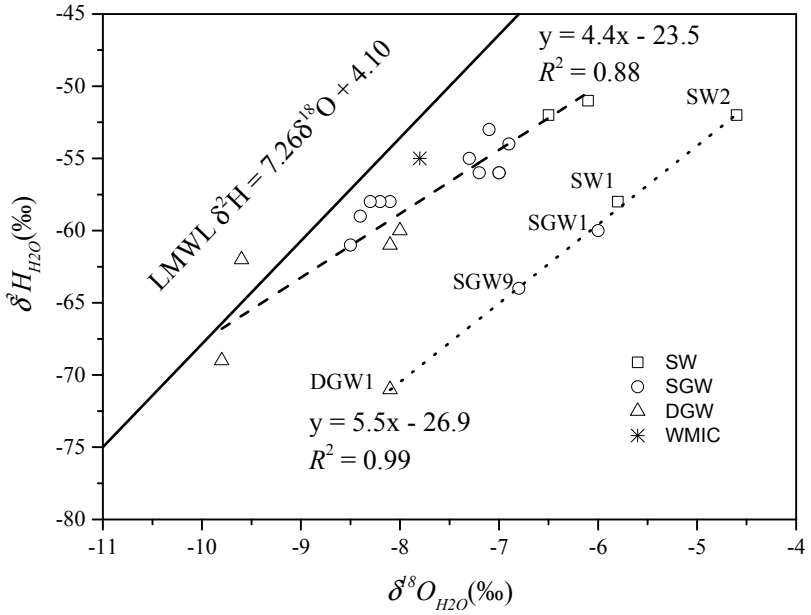

Figure 6. Plot of δ^2H against $\delta^{18}O_{H2O}$ for surface and ground water samples from the Shijiazhuang area. Local meteoric water line (LMWL, solid line) and evaporation lines (dashed line and dotted line) are shown for comparison. The LMWL is defined by Jia *et al*. [45]. (SW: Surface water; SGW: Shallow groundwater; DGW: Deep groundwater; WMIC: Weighted mean isotope composition).

The surface water and groundwater samples on the dashed line below LMWL, with d-excess values of −2.2‰ to +14.8‰, suggest these samples experienced minor evaporation. The two surface water samples from Huangbizhuang (SW1) and Hutuohe reservoirs (SW2), with d-excess values of −15.2‰ and −11.6‰, suggest long-term strong evaporation of Huangbizhuang and Hutuohe reservoirs under the semi-arid climate. The groundwater samples (SGW1 and SGW9) were collected near the Huangbizhuang and Hutuohe reservoirs, indicating the seepage from Huangbizhuang and Hutuohe reservoirs are the major source of this groundwater. The DGW1 could be recharged by Hutuo River in an old and cold period. As shown in Figure 7, some of the shallow groundwater samples have similar $\delta^{18}O_{H2O}$ values and Cl^- concentrations with the surface waters, suggesting that these samples can be recharged by the surface water. In addition, wastewater contributes a considerable amount of Cl^- to the shallow groundwater in the mixing process. Moreover, deep groundwater quality could be influenced by seepage from shallow groundwater. The surface water sample (SW2) might be subjected to intensive evaporation resulting in high Cl^- concentration and $\delta^{18}O_{H2O}$ value.

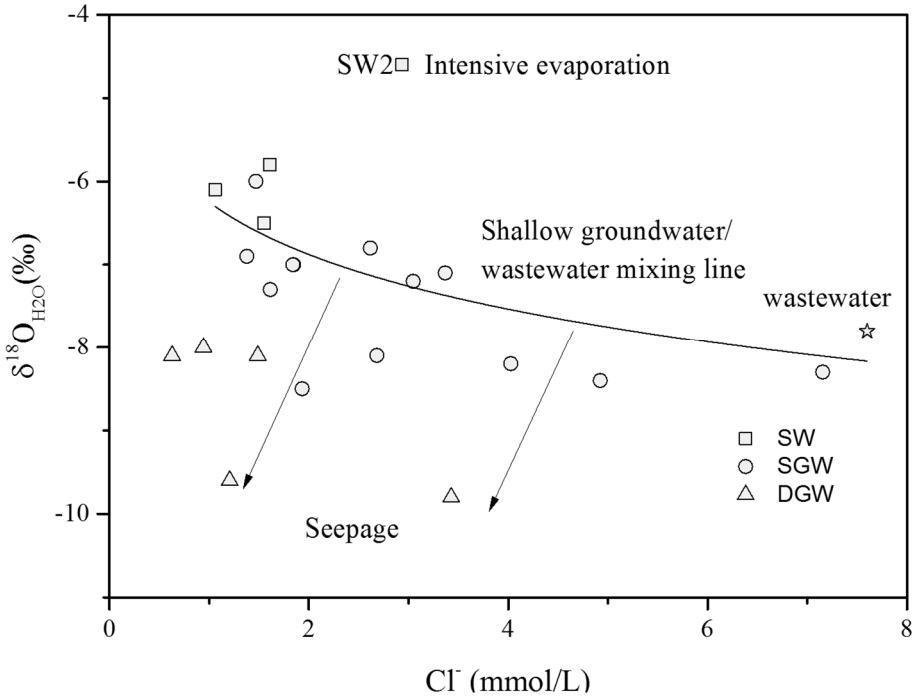

Figure 7. Cl^- concentrations *vs.* $\delta^{18}O_{H2O}$ values in the surface water and groundwater. (SW: Surface water; SGW: Shallow groundwater; DGW: Deep groundwater).

4.2. Source and Behavior of Nitrate

4.2.1. Evidence of Denitrification

Characterizing biogeochemical processes in groundwater is a key issue to understand the sources and behavior of NO_3^-. Microbial denitrification can decrease NO_3^- concentration and cause significant alterations of the isotopic composition of NO_3^-. Various studies have demonstrated that the heavy isotopes $^{15}N_{NO3}$ and $^{18}O_{NO3}$ become enriched with an εN/εO ratio that ranges from 1.3 to 2.1 in the residual NO_3^- pool during microbial denitrification [20,21,46,47]. Although the individual isotopic enrichment factors for $\delta^{15}N_{NO3}$ and $\delta^{18}O_{NO3}$ during denitrification may vary according to specific field conditions, the fractionation ratio (εN/εO) appears to remain constant. In this study, most of the samples show a positive trend in a $\delta^{15}N_{NO3}$ and $\delta^{18}O_{NO3}$ diagram (Figure 8) with an εN/εO ratio of proximately 2, suggesting microbial denitrification might occur. There were more positive $\delta^{15}N_{NO3}$ and $\delta^{18}O_{NO3}$ values and lower NO_3^- concentrations in deep groundwater than those in shallow groundwater (Figure 9a,b). This indicates that the higher extent of denitrification in the deep groundwater than that in the shallow groundwater.

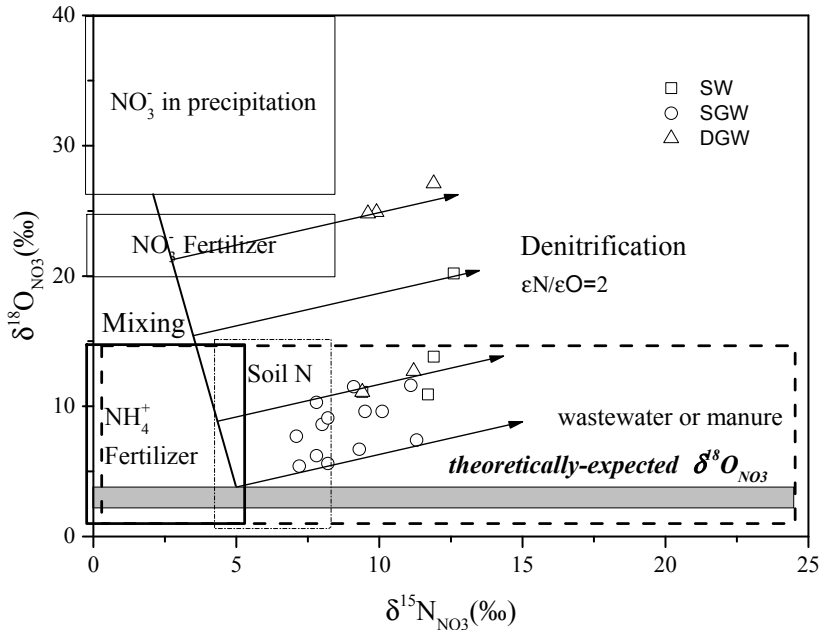

Figure 8. Isotopic values of surface water and groundwater dissolved NO_3^- plotted with the ranges of the potential NO_3^- sources in the study area [4,9,48]. (SW: Surface water; SGW: Shallow groundwater; DGW: Deep groundwater).

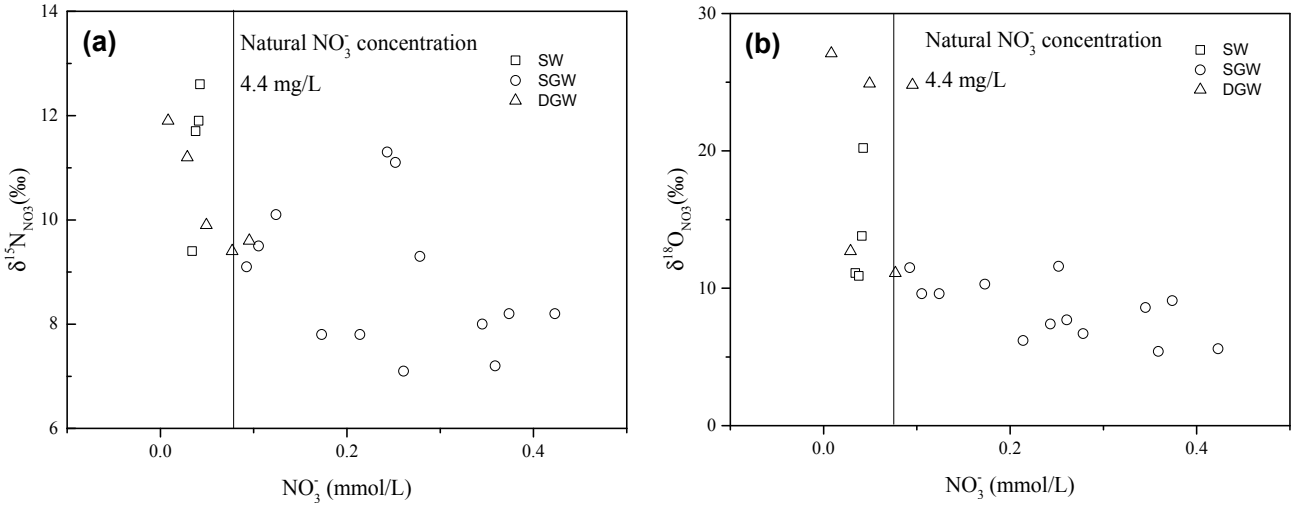

Figure 9. Relationship between isotopic composition of NO_3^- and NO_3^- concentration in the surface water and groundwater: (**a**) $\delta^{15}N_{NO3}$ *vs.* NO^-_3; (**b**) $\delta^{18}O_{NO3}$ *vs.* NO_3^- (SW: Surface water; SGW: Shallow groundwater; DGW: Deep groundwater).

Denitrification processes take place under reducing environments, usually in the saturated zone. This process is linked either to organic matter oxidation or sulfide oxidation [10,20,49]. It is believed that denitrification followed by sulfide oxidation cannot occur in carbonated aquifers where pH is over 7 [50]. Thus, DOC is the main energy source for microbial metabolism in the groundwater. The denitrification reaction involving carbon as electron donors can be described as follows:

$$5CH_2O + 4NO_3^- + 4H^+ \rightarrow 5CO_2 + 2N_2 + 7H_2O \quad (1)$$

For reaction (1), the residual DOC and NO_3^- will become increasingly enriched in the heavy isotopes (^{13}C and ^{15}N) rather than in the initial DOC and NO_3^- In the subsurface, a variety of biogeochemical reactions occur with DOC attenuation in the water infiltration and flow processes [22], while denitrification is the dominant attenuation process of NO_3^- in groundwater [10]. As shown in Figure 10, synergistic changes in $\delta^{13}C_{DOC}$ and $\delta^{15}N_{NO3}$ values of the groundwater samples imply that variation of $\delta^{15}N_{NO3}$ values are related to biogeochemical processes. It's reasonable to propose denitrification as the most possible process. SGW7 and SGW8, deviating from the positive relationship between $\delta^{13}C_{DOC}$ and $\delta^{15}N_{NO3}$ values, may be due to the import of manure ($\delta^{13}C_{DOC}$ = 27.3‰, [51]) in the Zhengding and Beigaoying areas where agricultural inputs could occur. Several samples (SGW9, DGW1, DGW5 and SW4) stray from the denitrification trend and approach SGW7 and SGW8, indicating these samples are concurrently influenced by the manure pollution and denitrification. The denitrification process occurs in the surface water (SW2) which has several favorable conditions such as low concentration of dissolved oxygen (2.3 mg/L) [23,28,52] and high concentration of DOC (22.1 mg C/L). The surface water with relatively high $\delta^{15}N_{NO3}$ values and low $\delta^{13}C_{DOC}$ values may be the result of preferential uptake of light nitrogen isotopes by algae, leading to enrichment of heavy nitrogen isotope in the residual NO_3^- [53–55]. In general, the high $\delta^{13}C_{DOC}$ and $\delta^{15}N_{NO3}$ values highlight that a limited extent of microbial denitrification occurred mainly in the deep groundwater and part of the shallow groundwater and surface water. The low concentration (typically < 5 mg C/L) and bioavailability of residual DOC may be one of the most important reasons for the low extent of denitrification in the study area [56].

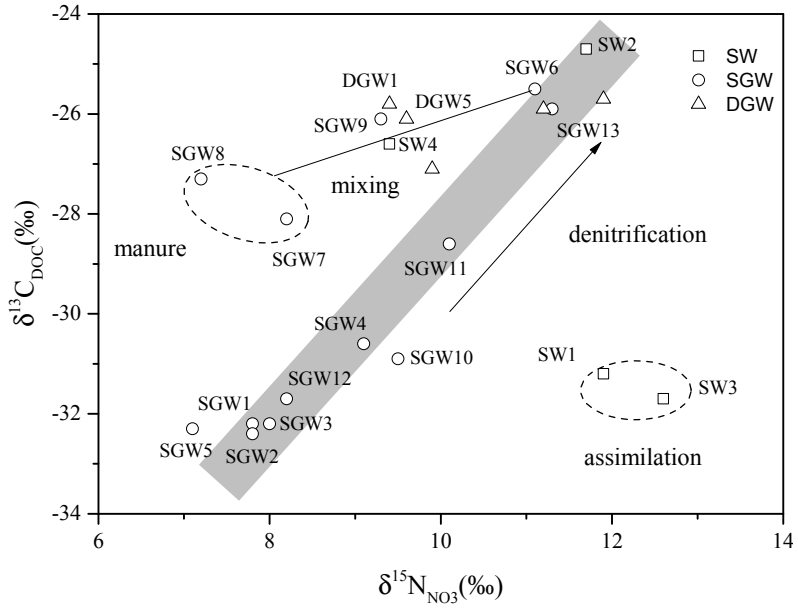

Figure 10. Plot of $\delta^{13}C_{DOC}$ and $\delta^{15}N_{NO3}$ in surface water and groundwater. The rectangle with gray shadow indicates the synergic trend between $\delta^{13}C_{DOC}$ and $\delta^{15}N_{NO3}$. The two ellipses with dashed lines highlight the values deviating from the trend due to mixing with different sources and assimilation by microbial activities. (SW: Surface water; SGW: Shallow groundwater; DGW: Deep groundwater).

4.2.2. Sources of NO_3^- in Groundwater

The possible sources of nitrate in the groundwater in this area include agricultural input including NO_3^- fertilizer, NH_4^+ fertilizer and manure, domestic and industrial wastewater, soil organic N, and atmospheric deposition. The characteristic N and O isotopic compositions of these possible nitrate sources are displayed in Figure 8.

In this study, denitrification poses the most difficulties for simple applications of nitrate isotopes. However, according to the mixing model reported in the previous study [9,57], combining the denitrification trend (εN/εO ratio) with the theoretically-expected $\delta^{18}O_{NO3}$ value could preliminarily deduce the initial $\delta^{15}N_{NO3}$ values of the NO_3^- in the water samples. In the case of the NO_3^- of groundwater originating from soil organic N, manure, NH_4^+ fertilizer and wastewater, the dominant process related to NO_3^- throughout the hydrochemical profile is nitrification. Generally, NO_3^- generated via microbial nitrification incorporates two oxygen atoms from water and one from atmospheric O_2 [58,59]. Therefore, the expected $\delta^{18}O$ value of NO_3^- may be estimated as follows:

$$\delta^{18}O_{NO3} = 2/3\delta^{18}O_{H2O} + 1/3\delta^{18}O_{O2} \quad (2)$$

The $\delta^{18}O$ signature of soil O_2 is equivalent to that of atmospheric O_2 which is about +23.5‰ [9]. The $\delta^{18}O_{H2O}$ of shallow groundwater in the investigated aquifer system ranges from −8.5‰ to −6.0‰ (Table 2). Consequently, the expected $\delta^{18}O_{NO3}$ value for groundwater NO_3^- derived from nitrification of alternative sources in soils should be in the range of +2.2‰ to +3.8‰. The theoretically-expected value is less than the measured $\delta^{18}O_{NO3}$ values (+5.4‰ to +9.1‰). Theoretically, both denitrification and contribution of NO_3^- in precipitation to natural water can lead to the increase in $\delta^{18}O_{NO3}$ values. In this study, if denitrification is the only process for the elevated $\delta^{18}O_{NO3}$ values, the initial $\delta^{15}N_{NO3}$ values of DGW samples should be extremely depleted (less than −20‰) which are deviated from the common values −10‰ to +20‰) [4] (Figure 8). Thus, the relatively high $\delta^{18}O_{NO3}$ values of DGW samples cannot be simply explained by the denitrification process, suggesting the existence of other process. As shown in Figure 8, denitrification, coupled with mixing processes between precipitation and surficial sources (soil organic N, wastewater, manure and NH_4^+ fertilizer) can be responsible for the higher $\delta^{18}O_{NO3}$ values of the water samples. In addition, the $\delta^{15}N_{NO3}$ value(s) of possible surficial source(s) can be roughly estimated between 2‰ and 5‰ according to the mixing model. The typical $\delta^{15}N_{NO3}$ values of soil N ranged from 0 to 8‰ and NH_4^+ fertilizers from −6‰ and +6‰ [4]. In the SJZ area, the $\delta^{15}N_{NO3}$ value of effluents N in the wastewater irrigated area was 2.5‰ [6], while the $\delta^{15}N_{NO3}$ value of NO_3^- in the unsaturated zone was 5.7‰ [7]. The reported values of $\delta^{15}N_{NO3}$ ranged between +8.7‰ and 14.4‰ for the compost-applied area and between +4.5‰ and +8.5‰ for the area where urea was applied with compost [12]. In general, soil N, NH_4^+ fertilizer, wastewater, and the mix of NH_4^+ fertilizer and manure could be possible NO_3^- sources.

For the shallow groundwater, soil organic N and precipitation cannot be the main origins of NO_3^- since NO_3^- concentrations of most samples are much higher than the natural NO_3^- concentration (4.4 mg/L [60]) (Figure 9a). Thus, NO_3^- in the shallow groundwater mainly derives from anthropogenic sources. In the non-wastewater-irrigated area, NH_4^+ fertilizer could be the dominant NO_3^- source due to the initial $\delta^{15}N_{NO3}$ values entirely falling in the range of NH_4^+ fertilizer. In the wastewater-irrigated area, wastewater is the primary NO_3^- source. The relatively low NO_3^-/Cl^- ratios of these samples collected

from the wastewater-irrigated area can be another important piece of evidence for wastewater sources (Figure 11). For the deep groundwater, the samples with relatively low $\delta^{18}O_{NO3}$ values might be contaminated by wastewater, while the samples with relatively high $\delta^{18}O_{NO3}$ values could be attributed to a mixture of precipitation and soil organic N contribution (Figure 8).

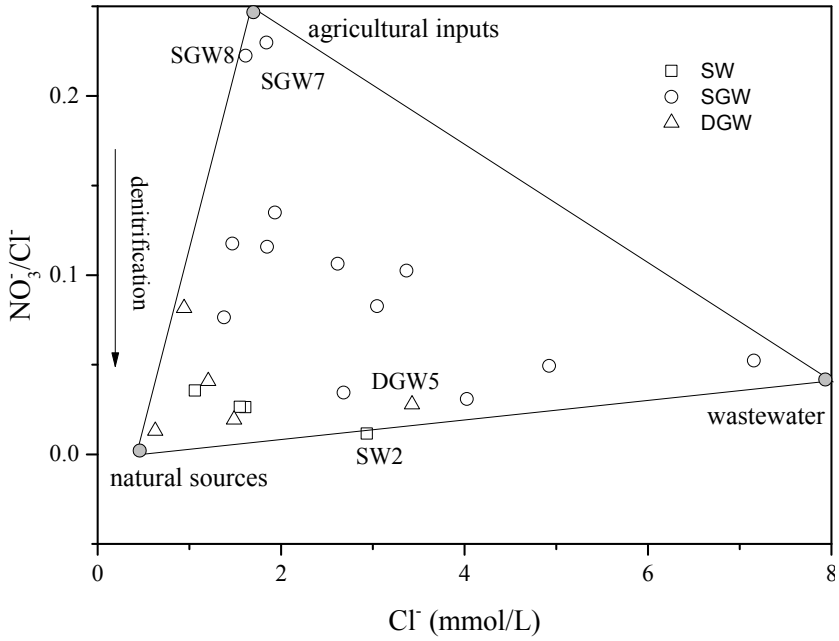

Figure 11. Variations of NO_3^- /Cl^- molar ratios with Cl^- molar concentrations of surface water and groundwater. The solid lines represent the theoretical mixing lines constructed by using the manure, municipal wastewater, and precipitation as end members. (SW: Surface water; SGW: Shallow groundwater; DGW: Deep groundwater).

The mixing of different NO_3^- sources can be characterized by the pattern of NO_3^- /Cl^- ratios and Cl concentrations (Figure 11). Agricultural inputs (high NO_3^-/Cl^- ratios and low Cl concentration) are the dominant NO_3^- sources in the Zhengding and Beigaoying areas. The samples collected from the southern part of the study area are characterized by lower NO_3^- /Cl^- ratios but high Cl^- concentrations, confirming that long-term wastewater irrigation has a significant impact on the groundwater quality [6]. The surface water and deep groundwater are both primarily originated from natural sources (precipitation and soil organic nitrogen) with little influence of anthropogenic activities, and show low NO_3^- /Cl^- ratios and Cl^- concentrations. However, the samples SW2 and DGW5 are polluted by wastewater and show increased Cl^- concentration. All data points are included in a mixing triangle, with end members represented by wastewater, natural sources, and agricultural inputs. Several points located in the middle of the mixing triangle, suggesting varied sources, can jointly aggravate the nitrate pollution.

5. Conclusions

This study focuses on the sources and fate of NO_3^- in the groundwater used as drinking water in the rural and suburban areas of SJZ, China.

The dissolution of the calcium carbonate and gypsum minerals was the most effective process in the groundwater chemistry. Hydrochemical data suggested that NO_3^- in the groundwater could be related

to wastewater irrigation or usage of fertilizers. The isotopic data ($\delta^{18}O$ and $\delta^{2}H$) indicated that the groundwater originated primarily from local precipitation and experiences different in extent of evaporation.

Denitrification affects the transformation of NO_3^- in the groundwater supported by the fractionation ratio ($\varepsilon N/\varepsilon O$) and the pattern of $\delta^{13}C_{DOC}$ and $\delta^{15}N_{NO3}$. Our study clarifies that a low extent of denitrification could be ubiquitous in the groundwater, and the effect of denitrification in the deep groundwater is more significant than that in the shallow groundwater.

For the shallow groundwater, NO_3^- contamination is predominantly derived from NH_4^+ fertilizers in non-wastewater irrigated areas; in contrast, the NO_3^- source can be mainly attributed to wastewater in wastewater irrigated area. For the deep groundwater samples, NO_3^- could primarily originate from precipitation and soil organic N. In addition, some of them were influenced by wastewater. In this study, the mixing processes of various NO_3^- sources are confirmed by dual isotopes ($\delta^{15}N_{NO3}$, and $\delta^{18}O_{NO3}$) and hydrochemistry (NO_3^-/Cl^- ratio and Cl concentration) in the drinking water wells of SJZ.

Acknowledgments

The authors thank the anonymous reviewers for constructive comments that greatly improved this manuscript. We are grateful to Editor Jun Xu for his constructive comments. This work was financially supported by the National Natural Science Foundation of China (NSFC Grant Nos. 41002083, 40972157, and 41202169).

Author Contributions

Yanpeng Zhang participated in field sampling, experiments, design of the study, and writing the manuscript. Aiguo Zhou and Jianwei Zhou are co-supervisors of this research who guided the research and contributed to preparing the manuscript for publication. Cunfu Liu and Hesheng Cai modified the discussion section and made improvements to the English writing of the manuscript as well. Yunde Liu and Wen Xu participated in the field sampling and the experiments.

Conflicts of Interest

The authors declare no conflict of interest.

References

1. Zhang, Z.; Shen, Z.; Xue, Y.; Ren, F.; Shi, D.; Yin, Z.; Zhong, Z.; Sun, X. *Evolution of Groundwater Environment in North China Plain*; Geological Publishing House: Beijing, China, 2000.
2. Zhang, Z.; Fei, Y.; Chen, Z.; Zonggu, Z.; Xie, Z.; Wang, Y. *Investigation and Evaluation of Groundwater Sustainable Utilization in North China Plain*; Geological Publishing House: Beijing, China, 2009.
3. Kendall, C.; Aravena, R. Nitrate isotopes in groundwater systems. In *Environmental Tracers in Subsurface Hydrology*; Springer: New York, NY, USA, 2000; pp. 261–297.
4. Xue, D.; Botte, J.; de Baets, B.; Accoe, F.; Nestler, A.; Taylor, P.; van Cleemput, O.; Berglund, M.; Boeckx, P. Present limitations and future prospects of stable isotope methods for nitrate source identification in surface- and groundwater. *Water Res.* **2009**, *43*, 1159–1170.

5. Fenech, C.; Rock, L.; Nolan, K.; Tobin, J.; Morrissey, A. The potential for a suite of isotope and chemical markers to differentiate sources of nitrate contamination: A review. *Water Res.* **2012**, *46*, 2023–2041.
6. Chen, J.Y.; Tang, C.Y.; Yu, J.J. Use of ^{18}O, ^{2}H and ^{15}N to identify nitrate contamination of groundwater in a wastewater irrigated field near the city of Shijiazhuang, China. *J. Hydrol.* **2006**, *326*, 367–378.
7. Liu, J.; Chen, Z.Y. Using stable isotope to trace the sources of nitrate in groundwater in Shijiazhuang. *Chin. J. Environ. Sci.* **2009**, *30*, 1602–1607.
8. Zhang, C.Y.; Zhang, S.; Ma, L.N.; Yin, M. Nitrogen isotope tracing of sources of nitrate contamination in groundwater from wastewater irrigated area. *Earth Sci.* **2012**, *37*, 350–356.
9. Kendall, C.; MacDonnell, J.J. *Isotope Tracers in Catchment Hydrology*; Access Online via Elsevier: Amsterdam, Noord-Holland, The Netherlands, 1998.
10. Rivett, M.O.; Buss, S.R.; Morgan, P.; Smith, J.W.; Bemment, C.D. Nitrate attenuation in groundwater: A review of biogeochemical controlling processes. *Water Res.* **2008**, *42*, 4215–4232.
11. Choi, W.J.; Lee, S.M.; Ro, H.M. Evaluation of contamination sources of groundwater NO_3^- using nitrogen isotope data: A review. *Geosci. J.* **2003**, *7*, 81–87.
12. Choi, W.-J.; Han, G.-H.; Lee, S.-M.; Lee, G.-T.; Yoon, K.-S.; Choi, S.-M.; Ro, H.-M. Impact of land-use types on nitrate concentration and $\delta^{15}N$ in unconfined groundwater in rural areas of Korea. *Agric. Ecosyst. Environ.* **2007**, *120*, 259–268.
13. Widory, D.; Kloppmann, W.; Chery, L.; Bonnin, J.; Rochdi, H.; Guinamant, J.L. Nitrate in groundwater: An isotopic multi-tracer approach. *J. Contam. Hydrol.* **2004**, *72*, 165–188.
14. Mongelli, G.; Paternoster, M.; Sinisi, R. Assessing nitrate origin in a volcanic aquifer using a dual isotope approach. *Int. J. Environ. Sci. Technol.* **2013**, *10*, 1149–1156.
15. Thurman, E.M. *Organic Geochemistry of Natural Waters*; Springer: Dordrecht, The Netherlands, 1985; Volume 2.
16. Hartland, A.; Fenwick, G.D.; Bury, S.J. Tracing sewage-derived organic matter into a shallow groundwater food web using stable isotope and fluorescence signatures. *Mar. Freshwater Res.* **2011**, *62*, 119–129.
17. Starr, R.C.; Gillham, R.W. Denitrification and organic carbon availability in two aquifers. *Ground Water* **1993**, *31*, 934–947.
18. Nishikawa, T.; District, H.D.W. *Evaluation of the Source and Transport of High Nitrate Concentrations in Ground Water, Warren Subbasin, California*; US Department of the Interior, US Geological Survey: Sacramento, CA, USA, 2003.
19. Cannavo, P.; Richaume, A.; Lafolie, F. Fate of nitrogen and carbon in the vadose zone: *In situ* and laboratory measurements of seasonal variations in aerobic respiratory and denitrifying activities. *Soil Biol. Biochem.* **2004**, *36*, 463–478.
20. Fukada, T.; Hiscock, K.M.; Dennis, P.F.; Grischek, T. A dual isotope approach to identify denitrification in groundwater at a river-bank infiltration site. *Water Res.* **2003**, *37*, 3070–3078.
21. Aravena, R.; Robertson, W.D. Use of multiple isotope tracers to evaluate denitrification in ground water: Study of nitrate from a large—Flux septic system plume. *Ground Water* **1998**, *36*, 975–982.
22. Pabich, W.J.; Valiela, I.; Hemond, H.F. Relationship between DOC concentration and vadose zone thickness and depth below water table in groundwater of Cape Cod, USA. *Biogeochemistry* **2001**, *55*, 247–268.

23. Desimone, L.A.; Howes, B.L. Nitrogen transport and transformations in a shallow aquifer receiving wastewater discharge: A mass balance approach. *Water Resour. Res.* **1998**, *34*, 271–285.
24. Rivett, M.O.; Smith, J.W.N.; Buss, S.R.; Morgan, P. Nitrate occurrence and attenuation in the major aquifers of England and Wales. *Q. J. Eng. Geol. Hydrogeol.* **2007**, *40*, 335–352.
25. Kortelainen, N.M.; Karhu, J.A. Tracing the decomposition of dissolved organic carbon in artificial groundwater recharge using carbon isotope ratios. *Appl. Geochem.* **2006**, *21*, 547–562.
26. Mohammadzadeh, H.; Clark, I. Bioattenuation in groundwater impacted by landfill leachate traced with $\delta^{13}C$. *Ground Water* **2011**, *49*, 880–890.
27. Van Breukelen, B.M.; Roling, W.F.M.; Groen, J.; Griffioen, J.; van Verseveld, H.W. Biogeochemistry and isotope geochemistry of a landfill leachate plume. *J. Contam. Hydrol.* **2003**, *65*, 245–268.
28. Mengis, M.; Schiff, S.L.; Harris, M.; English, M.C.; Aravena, R.; Elgood, R.J.; MacLean, A. Multiple geochemical and isotopic approaches for assessing ground water NO_3^- elimination in a riparian zone. *Ground Water* **1999**, *37*, 448–457.
29. Widory, D.; Petelet-Giraud, E.; Negrel, P.; Ladouche, B. Tracking the sources of nitrate in groundwater using coupled nitrogen and boron isotopes: A synthesis. *Environ. Sci. Technol.* **2005**, *39*, 539–548.
30. Liu, C.Q.; Li, S.L.; Lang, Y.C.; Xiao, H.Y. Using $\delta^{15}N$ and $\delta^{18}O$ values to identify nitrate sources in Karst ground water, Guiyang, southwest China. *Environ. Sci. Technol.* **2006**, *40*, 6928–6933.
31. Chen, W.H. *Groundwater in Hebei*; Seismological Press: Beijing, China, 1999.
32. Lu, Y.T.; Tang, C.Y.; Chen, J.Y.; Song, X.F.; Li, F.D.; Sakura, Y. Spatial characteristics of water quality, stable isotopes and tritium associated with groundwater flow in the hutuo river alluvial fan plain of the north China plain. *Hydrogeol. J.* **2008**, *16*, 1003–1015.
33. Wu, C.; Xu, Q.H.; Ma, Y.H.; Zhang, X.Q. Palaeochannels on the north China plain: Palaeoriver geomorphology. *Geomorphology* **1996**, *18*, 37–45.
34. Chen, Z.Y.; Nie, Z.L.; Zhang, Z.J.; Qi, J.X.; Nan, Y.J. Isotopes and sustainability of ground water resources, north China plain. *Ground Water* **2005**, *43*, 485–493.
35. Yang, Y.; Watanabe, M.; Sakura, Y.; Changyuan, T.; Hayashi, S. Groundwater-table and recharge changes in the piedmont region of Taihang mountain in gaocheng city and its relation to agricultural water use. *WaterSA* **2004**, *28*, 171–178.
36. Li, W. Research of Environment Evolution of Groundwater in Shijiazhuang. Master's Thesis, Shijiazhuang University of Economics, Shijiazhuang, China, June 2009.
37. Liu, C.M.; Yu, J.J.; Kendy, E. Groundwater exploitation and its impact on the environment in the north China plain. *Water Int.* **2001**, *26*, 265–272.
38. Chen, J.Y.; Tang, C.Y.; Shen, Y.J.; Sakura, Y.; Kondoh, A.; Shimada, J. Use of water balance calculation and tritium to examine the dropdown of groundwater table in the piedmont of the north China plain (NCP). *Environ. Geol.* **2003**, *44*, 564–571.
39. Liu, J.; Zheng, C.; Zheng, L.; Lei, Y. Ground water sustainability: Methodology and application to the north China plain. *Ground Water* **2008**, *46*, 897–909.
40. Liu, Y.D.; Gan, Y.Q.; Yu, T.T.; Liu, C.F.; Zhou, A.G. Online simultaneous determination of δD and $\delta^{18}O$ in microliter water samples by thermal conversion/elemental analysis isotope ratio mass spectrometry. *China Rock Min. Anal.* **2010**, *29*, 643–647.

41. Silva, S.; Kendall, C.; Wilkison, D.; Ziegler, A.; Chang, C.; Avanzino, R. A new method for collection of nitrate from fresh water and the analysis of nitrogen and oxygen isotope ratios. *J. Hydrol.* **2000**, *228*, 22–36.
42. Gandhi, H.; Wiegner, T.N.; Ostrom, P.H.; Kaplan, L.A.; Ostrom, N.E. Isotopic (^{13}C) analysis of dissolved organic carbon in stream water using an elemental analyzer coupled to a stable isotope ratio mass spectrometer. *Rapid Commun. Mass Spectrom.* **2004**, *18*, 903–906.
43. Appelo, C.A.J.; Postma, D. *Geochemistry, Groundwater and Pollution*; CRC Press: Leiden, The Netherlands, 2005.
44. Dejwakh, N.R.; Meixner, T.; Michalski, G.; McIntosh, J. Using ^{17}O to investigate nitrate sources and sinks in a semi-arid groundwater system. *Environ. Sci. Technol.* **2012**, *46*, 745–751.
45. Jia, G.; Yu, X.; Fan, D.; Zheng, J. Study on hydrogen and oxygen stable isotopes in precipitation in both sides along Taihang mountain. *Yellow River* **2011**, *7*, 34–36.
46. Böttcher, J.K.; Strebel, O.; Voerkelius, S.; Schmidt, H.L. Using isotope fractionation of nitrate-nitrogen and nitrate-oxygen for evaluation of microbial denitrification in a sandy aquifer. *J. Hydrol.* **1990**, *114*, 413–424.
47. Wassenaar, L.I. Evaluation of the origin and fate of nitrate in the abbotsford aquifer using the isotopes of ^{15}N and ^{18}O in NO_3^- . *Appl. Geochem.* **1995**, *10*, 391–405.
48. Heaton, T. Isotopic studies of nitrogen pollution in the hydrosphere and atmosphere: A review. *Chem. Geol.* **1986**, *59*, 87–102.
49. Vitoria, L.; Soler, A.; Canals, A.; Otero, N. Environmental isotopes (N, S, C, O, D) to determine natural attenuation processes in nitrate contaminated waters: Example of Osona (NE Spain). *Appl. Geochem.* **2008**, *23*, 3597–3611.
50. Otero, N.; Torrento, C.; Soler, A.; Mencio, A.; Mas-Pla, J. Monitoring groundwater nitrate attenuation in a regional system coupling hydrogeology with multi-isotopic methods: The case of Plana de Vic (Osona, Spain). *Agric. Ecosyst. Environ.* **2009**, *133*, 103–113.
51. Senbayram, M.; Dixon, L.; Goulding, K.W.; Bol, R. Long—Term influence of manure and mineral nitrogen applications on plant and soil ^{15}N and ^{13}C values from the Broadbalk Wheat Experiment. *Rapid. Commun. Mass Spectrom.* **2008**, *22*, 1735–1740.
52. Beller, H.R.; Madrid, V.; Hudson, G.B.; McNab, W.W.; Carlsen, T. Biogeochemistry and natural attenuation of nitrate in groundwater at an explosives test facility. *Appl. Geochem.* **2004**, *19*, 1483–1494.
53. Johannsen, A.; Dähnke, K.; Emeis, K. Isotopic composition of nitrate in five German rivers discharging into the North Sea. *Org. Geochem.* **2008**, *39*, 1678–1689.
54. Battaglin, W.A.; Kendall, C.; Chang, C.C.; Silva, S.R.; Campbell, D. Chemical and isotopic evidence of nitrogen transformation in the mississippi river, 1997–98. *Hydrol. Process* **2001**, *15*, 1285–1300.
55. Albertin, A.R.; Sickman, J.O.; Pinowska, A.; Stevenson, R.J. Identification of nitrogen sources and transformations within Karst springs using isotope tracers of nitrogen. *Biogeochemistry* **2012**, *108*, 219–232.
56. Baker, M.A.; Vervier, P. Hydrological variability, organic matter supply and denitrification in the Garonne river ecosystem. *Freshw. Biol.* **2004**, *49*, 181–190.

57. Kendall, C.; Campbell, D.H.; Burns, D.A.; Shanley, J.B.; Silva, S.R.; Chang, C.C. Tracing sources of nitrate in snowmelt runoff using the oxygen and nitrogen isotopic compositions of nitrate. In *International Symposium on Biogeochemistry of Seasonally Snow-Covered Catchments*, Boulder, CO, USA, 1–14 July 1995; Tonnessen, K.A., Williams, M.W., Tranter, M., Eds.; International Association of Hydrological Sciences: Wallingford, UK; Volume 228, pp. 339–347.
58. Andersson, K.K.; Hooper, A.B. O_2 and H_2O are each the source of one o in NO_2^- produced from NH_3 by *Nireosomonas* ^{15}N-NMR evidence. *FEBS Lett.* **1983**, *164*, 236–240.
59. Snider, D.M.; Spoelstra, J.; Schiff, S.L.; Venkiteswaran, J.J. Stable oxygen isotope ratios of nitrate produced from nitrification: ^{18}O-Labeled water incubations of agricultural and temperate forest soils. *Environ. Sci. Technol.* **2010**, *44*, 5358–5364.
60. Li, Z.H.; Wang, D.S. Impact of human activities on nitrate concentration in the shallow groundwater. *Site Invest. Sci. Technol.* **1999**, *1*, 37–41.